Construction and Building Materials 189 (2018) 736–744

Contents lists available at ScienceDirect

Construction and Building Materials

journal homepage: www.elsevier.com/locate/conbuildmat

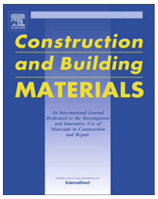

# Shrinkage-free tension stiffening law for various concrete grades

Gintaris Kaklauskas *, Vytautas Tamulenas, Mattia Francesco Bado, Darius Bacinskas

*Department of Reinforced Concrete Structures and Geotechnics, Vilnius Gediminas Technical University, Sauletekio al. 11, LT-10223 Vilnius, Lithuania*

## HIGHLIGHTS

- The shrinkage effect drastically changes the shape of tension stiffening relations.
- A shrinkage-free tension stiffening law for reinforced concrete ties was proposed.
- An extensive database (108 members) ensures the universal applicability of the law.
- The prediction results were validated against independent test data.

## ARTICLE INFO

*Article history:*
Received 9 March 2018
Received in revised form 24 July 2018
Accepted 31 August 2018
Available online 17 September 2018

*Keywords:*
Reinforced concrete tension members
Tension stiffening
Shrinkage effect

## ABSTRACT

The present study proposes a new tension stiffening law for reinforced concrete (RC) that takes into account the shrinkage effect occurring prior to the external loading. Due to the restraining action of reinforcement, shrinkage induces tension stresses in the concrete which may significantly reduce the crack resistance and increase deformations of the RC member. The proposed tension stiffening model is based on the test data of seven experimental programs reported in the literature, including 108 RC tension members covering a wide range of concrete grade, reinforcement ratio and bar diameter. The study has shown that shrinkage drastically changes the shape of tension stiffening relations with reinforcement ratio being the most important parameter responsible for this effect. This study reports a limited validation analysis of the proposed constitutive law based on experimental data reported herein. For that tests on four tensile RC members with measured free shrinkage strain have been carried out. The comparative analysis has shown good agreement between the experimental and predicted load–strain and tension stiffening relations.

## 1. Introduction

Reinforced concrete (RC) is an exceptional structural material due to two aspects: the extent of its practical use and the complexity of its mechanical behaviour. The latter characterisation is attributed to such phenomena as concrete shrinkage and creep as well as cracking, tension softening and tension stiffening, all being highly interrelated with each other. Tension softening is a property of plain concrete to transmit tensile stresses in the cracked section whereas tension stiffening is the ability of concrete to carry tensile stresses in the sections between cracks due to the bond action with reinforcement. Tension stiffening parameters have a significant effect on numerical results of deformation and crack analysis [1,2] of RC structures.

Recently, a new concept of crack analysis of reinforced concrete members has been proposed in [3,4]. The philosophy behind the proposed methodology is to establish mean spacing between primary cracks through the compatibility of the stress-transfer and mean deformation approaches. Parameters of crack spacing are obtained by equating the mean strains of the tensile reinforcement defined by these approaches. The technique considers a single RC block of a length of the mean crack spacing assuming that it represents the averaged deformation behaviour of a cracked member. Based on the experimental evidence, the reinforcement strain within the block is characterized by a strain profile consisting of straight lines. The model was shown to be a simple and mechanically sound tool for predicting mean crack spacing of RC members. However, a comparative analysis of the predictions to the test data has shown that the accuracy of the proposed approach of crack analysis is strongly dependent on the adequacy of the assumed tension stiffening model as it significantly affects the deformations in the tensile reinforcement [4].

A number of approaches have been proposed to take into account the tension stiffening effect in the serviceability analysis of RC structures [5–13]. The *stress-transfer* approach based on the

---

* Corresponding author.
*E-mail address:* Gintaris.Kaklauskas@vgtu.lt (G. Kaklauskas).

https://doi.org/10.1016/j.conbuildmat.2018.08.212
0950-0618/

bond-slip interaction between concrete and reinforcement most realistically deals with discrete cracking phenomenon [3,6,9,11]. However, lack of adequate bond-slip models and complex mechanisms of analysis limit a wider application of the latter approach. Models with *smeared* (averaged) representation of deformations and cracks due to their simplicity are most extensively used in the numerical applications [5,7–10,12]. In the *smeared crack* approach, tension stiffening can be attributed either to concrete [7,8,12] or reinforcement [5,10]. Gribniak et al. [12] has proposed a stochastic approach in assessing tension stiffening. A simplified approach suggested by Eurocode 2 [13] based on the interpolation formula relating non-cracked and fully cracked states is frequently applied for the deformation analysis of RC ties. However, a statistical analysis [14] has shown that Eurocode 2 provides a far too stiff deformation response, particularly for lightly reinforced members. The prediction errors at various load levels ranged from 25 to 61% for lightly reinforced tensile members ($\rho$ <1.6%) and from 14 to 30% for the members with larger amounts of reinforcement ($\rho \geq$1.6%). As was shown in [14], the above inaccuracies to a significant extent were due to the shrinkage effect occurring prior to loading that was not taken into account by the Eurocode 2 [13]. Due to the restraining action of reinforcement or supports, shrinkage induces tension stresses in the concrete, which might significantly reduce crack resistance and increase deformations of the member [15]. Investigations [16–21] have shown that shrinkage may indeed have a significant effect on deformations of RC members subjected to short-term loading. However, very few tension stiffening models were proposed [16] that take into account or remove the shrinkage effect before calibrating the model; moreover, such models were generally based on a limited amount of test data. Recent investigations of tension stiffening [22–26] were mainly dedicated to new types of concrete and reinforcement.

The present study aims at proposing a new tension stiffening law being derived from a large amount of test data reported in the literature. The test data covers a wide range of geometrical and material properties such as concrete grade, reinforcement ratio and bar diameter. The proposed tension stiffening relationship has the removed shrinkage effect occurring prior to the external loading. The study reports a limited independent validation analysis of the proposed constitutive law based on experimental data reported herein.

## 2. Test data employed for deriving tension stiffening model

The new model is based on the test data of 7 experimental programs [27–33], listed in Table 1, which involved 108 RC elements (2800 measurements) having different concrete compressive strength up to 70 MPa. In addition to the compressive strength of concrete, the experimental programs covered a wide range of geometrical characteristics such reinforcement ratio and diameter of reinforcement bars. All the experimental programs involved prismatic specimens with nominally square sections reinforced by a single bar subjected to short-term axial tension. The specimens were tested either by controlling the deformations, as adopted in programs No. 1–5, or alternatively, controlling the applied tensile force, as adopted in programs No. 6 and 7.

The main characteristics of the specimens are given in Table 1. The first four columns refer to the test program number, the literature source of the program, the numbers of the tested elements, and the number of measurements in this program, respectively. Further parameters in Table 1 are: the actual height ($h$) and width ($b$) of the section; the concrete cover ($c$); the length of the specimen ($L$); the diameter of reinforcement bars ($D$); the area of reinforcement ($A_s$); the reinforcement ratio ($\rho$); the cylinder ($\varnothing 150 \times 300$ mm) strength ($f_c$); and the shrinkage strain ($\varepsilon_{cs}$) measured at the age of testing. When the values of the parameters varied within a range, the range of values rather than individual values are stated in the table. In the cases when the experimental shrinkage strain $\varepsilon_{cs}$ was not reported, it was assessed by the Eurocode 2 provisions using available test characteristics responsible for shrinkage.

The material characteristics needed for the analysis such as concrete tensile strength and modulus of elasticity were defined at the time of the short-term tests by the Eurocode 2 provisions based on the compressive strength:

$$f_{ct} = 0.3 \cdot (f_c - 8)^{(2/3)} \text{ when } f_c \leq 58 \text{ MPa} \tag{1a}$$

$$f_{ct} = 2.12 \cdot \ln(1 + (f_c/10)) \text{ when } f_c > 58 \text{ MPa} \tag{1b}$$

$$E_c = 22000 \cdot (f_c/10)^{0.3} \text{ [MPa]} \tag{2}$$

## 3. Basic equations for deriving tension stiffening stresses

The current analysis is based on smeared crack concept where stress in concrete is taken as the average tensile stress due to tension softening and the bond action between concrete and reinforcement bar, herein collectively called the tension stiffening. Based on the strain compatibility, it is assumed that

$$\varepsilon_m = \varepsilon_s = \varepsilon_{ct} \tag{3}$$

where $\varepsilon_m, \varepsilon_s$ and $\varepsilon_{ct}$ are the mean strains of the RC member, reinforcement and concrete, respectively.

The tension stiffening stress–strain relations can be obtained from load–strain diagrams of the experimental specimens (Table 1). Based on the equilibrium of internal forces and the external load,

$$P = N_s + N_c \tag{4}$$

where the internal forces acting in reinforcement, $N_s$, and concrete, $N_c$, are assessed as follows:

$$N_s = \varepsilon_s A_s E_s \tag{5}$$

$$N_c = \sigma_{ct} A_c \tag{6}$$

Then from Eqs. (3)–(6), the average tensile stress in concrete can be expressed as:

**Table 1**
Main characteristics of the test specimens used for the constitutive modelling.

| *No.* | *Reference* | *No. of elements* | *n* | $h$ | $b$ | $c$ | $L$ | $D$ | $A_s$ | $\rho$ | $f_c$ | $\varepsilon_{cs}$ |
|---|---|---|---|---|---|---|---|---|---|---|---|---|
| | | | | mm | | | | | mm$^2$ | % | MPa | μm/m |
| 1 | Farra and Jaccoud (1993) | 1–94 | 2184 | 100 | 100 | 40–45 | 1150 | 10–20 | 79–314 | 0.8–3.2 | 35.4–68.8 | – |
| 2 | Wu and Gilbert (2008) | 95–98 | 264 | 100 | 100 | 42–44 | 1100 | 12–16 | 113–201 | 1.1–2.1 | 21.6–24.7 | 28–249 |
| 3 | Choi and Maekawa (2003) | 99–102 | 106 | 100 | 100 | 42 | 1470 | 16 | 201 | 2.1 | 35.1–40.5 | – |
| 4 | Noghabai (2000) | 103–104 | 91 | 80–112 | 80–112 | 32–48 | 960 | 16 | 201 | 1.6–3.2 | 45.6 | – |
| 5 | Stroband (1991) | 105–106 | 69 | 100 | 100 | 42–44 | 935 | 12–16 | 113–201 | 1.1–2.1 | 49.6 | – |
| 6 | Scott and Gill (1987) | 107 | 51 | 103 | 101 | 46 | 1500 | 12 | 86 | 0.8 | 36.0 | – |
| 7 | Lorrain et al. (1998) | 108 | 35 | 100 | 100 | 44 | 2000 | 12 | 113 | 1.1 | 42.0 | – |

$$\sigma_{ct} = (P - \varepsilon_{ct} E_s A_s)/A_c \tag{7}$$

Figs. 1 and 2 illustrate the derivation of the tension stiffening relations from test load–strain diagrams of two singly reinforced concrete members reported in the test program by Farah and Jaccoud [27]. The members share the same cross-section and cylinder strength $f_c = 36.8$ MPa, but differ in the bar diameter (10 and 20 mm) and, therefore, in reinforcement ratio (0.8 and 3.2%). The solid lines in Fig. 1 show the experimental load–strain diagrams. The stress–strain tension stiffening relations calculated by Eqs. (3)–(7) are given in Fig. 2, a. It can be clearly seen that the member with larger reinforcement ratio possesses significantly lower tension stiffening stresses. It has been shown in [1,17] that such differences to a significant extent are caused by the influence of shrinkage effect. Next section discusses the influence of concrete shrinkage on deformations and tension stiffening of RC members.

## 4. Effect of shrinkage on deformations and tension stiffening

Concrete specimens can experience significant amounts of drying and autogenous shrinkage. Free shrinkage strain, $\varepsilon_{cs}$, depends on a number of characteristics such as time, ambient humidity, temperature, mixture proportions, material properties, curing conditions, and geometry of the element. Due to the non-uniform moisture distribution, the external layers of the member shrink more than the internal ones. This causes the non-uniform stress state throughout the section resulting in tension stresses in the exterior part and compression stresses in the mid area. Such effect is more characteristic to large elements with drying shrinkage confined to the external part of the section. For the smaller sections, as it is in the current study, it can be assumed that the member shrinks uniformly and will have no stresses, providing it has no restraint due to supports or reinforcement. Reinforcement bars placed in the member will provide restraint to shrinkage resulting in compressive stresses in the reinforcement and tensile stresses in the concrete [15]. Due to long-term action of the restraint, concrete stresses are relieved by creep. The effect of variation of concrete stress and modulus of elasticity in time can be taken into account by the ageing coefficient $\chi$ [15].

In the past, shrinkage has been generally neglected in predicting the deformation response of RC members. However, failure to account for the shrinkage effect may lead to inaccuracies in assessing member's crack resistance and stress–strain state. The latter can be predicted based on the principles of equilibrium and strain compatibility [15]. Alternatively, the shrinking effect can be taken into account by a fictitious force having the adequate effect on deformations of the member [17,18]. The fictitious force has to be of such a magnitude as to impose the free shrinkage strain, $\varepsilon_{cs}$, in the plain concrete specimen. Thus, the fictitious force is expressed through deformation modulus, $E_{ca}$, and cross-sectional area of concrete, $A_c$:

$$P_{cs}(t,t_0) = \varepsilon_{cs}(t,t_0)E_{ca}(t,t_0)A_c \tag{8}$$

where the age-adjusted effective modulus of concrete, $E_{ca}(t,t_0)$, is related to the creep factor $\varphi(t,t_0)$ and the ageing coefficient $\chi(t,t_0)$

$$E_{ca}(t,t_0) = E_c(t_0)/(1+\varphi(t,t_0)\chi(t,t_0)) \tag{9}$$

Here $E_c(t_0)$ is the modulus of elasticity of concrete; $t$ is the time under consideration; $t_0$ is the time of loading. Note that shrinkage strain, $\varepsilon_{cs}$, is taken negative.

The fictitious shrinkage force is applied at the centroid of the plain concrete section. In the general case of the centroids of plain concrete and RC sections not coinciding, the fictitious shrinkage force acts with eccentricity. In the case of tensile RC member

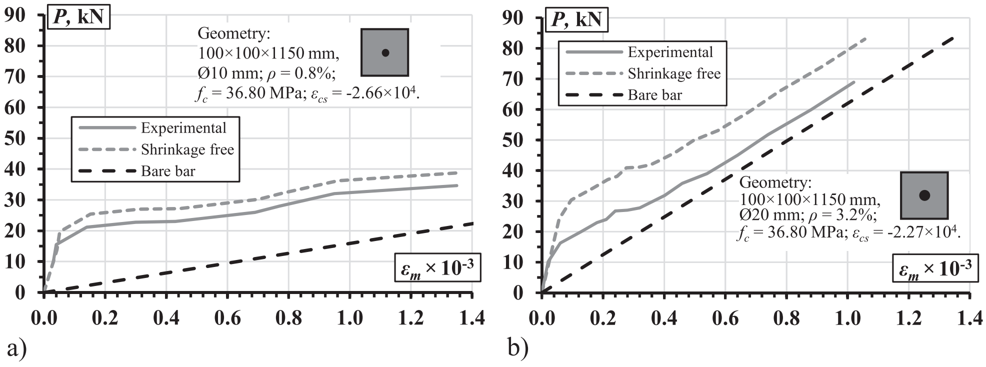

**Fig. 1.** Shrinkage effect on deformations of RC tension members [27] with different reinforcement ratio.

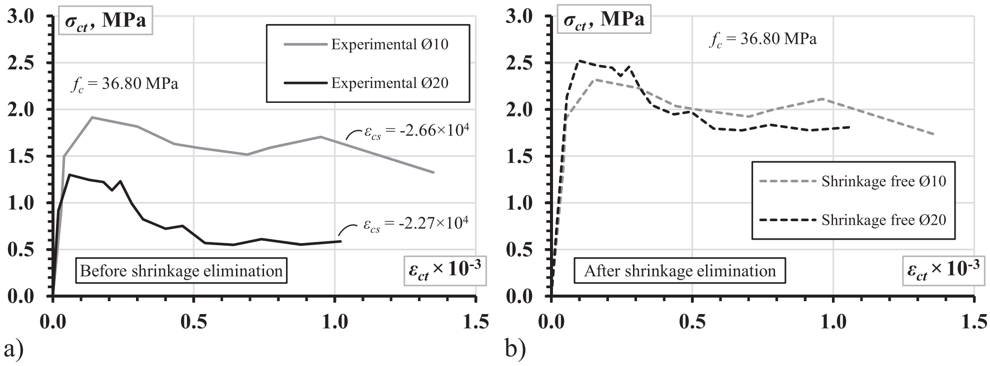

**Fig. 2.** Tension stiffening diagrams for RC tension members [27] with different reinforcement ratio.

having a symmetrical section, the shrinkage-induced longitudinal strain is calculated by this formula:

$$\varepsilon_{m,cs}(t,t_0) = \frac{P_{cs}(t,t_0)}{E_{ca}(t,t_0)A_c + E_sA_s} = \frac{\varepsilon_{cs}(t,t_0)E_{ca}(t,t_0)A_c}{E_{ca}(t,t_0)A_c + E_sA_s} = \frac{\varepsilon_{cs}(t,t_0)}{1 + \frac{E_s}{E_{ca}(t,t_0)}\rho} \qquad (10)$$

where $A_s$ is the area of reinforcement; $E_s$ is the modulus of elasticity of reinforcement.

From equilibrium, the internal forces acting in the concrete and reinforcement are equal in magnitude and opposite in sign. Shrinkage-induced tensile stress in concrete can be calculated by the formula [17]:

$$\sigma_{ct,cs}(t,t_0) = -\frac{\varepsilon_{cs}(t,t_0)E_s\rho}{1 + \frac{E_s}{E_{ca}(t,t_0)}\rho} \qquad (11)$$

Here $\rho = A_s/A_c$ is the reinforcement ratio.

The techniques to remove the shrinkage effect from load-deformation and tension stiffening relations have been proposed by Bischoff [1] and Kaklauskas and Gribniak [34]. The latter approach is more general as it is applicable not only to tensile members, but also to a combined action of axial force and bending moment. As was shown in [17], the removal of the shrinkage effect from tension stiffening relations of tensile RC members can be performed in a simple way by lifting up the stress–strain diagram by stress $\sigma_{ct,cs}$. Such stress modification for the two earlier discussed RC members with different reinforcement ratio is illustrated in Fig. 2(a). The shrinkage-induced tensile stresses calculated by Eq. (11) equaled to 0.406 and 1.224 MPa for the members reinforced with Ø10 and Ø20 bars, respectively. The stresses clearly depend on the reinforcement ratio with the larger value being in the member with higher amount of reinforcement. Addition of tension stiffening stresses shown in Fig. 2(a) and stresses $\sigma_{ct,cs}$ resulted in modified shrinkage-free tension stiffening relations that are presented in Fig. 2(b). In the modified stress–strain relations, the original values of strains were increased by $\sigma_{ct,cs}/E_c$. After the exclusion of shrinkage effect, the resulting curves have clearly approached each other indicating that tension stiffening effect is similar for the members with different reinforcement ratio.

In a similar way, the experimental load–strain curves of the RC ties were adjusted to eliminate the shrinkage effect. For that, the resultants of the shrinkage-free tension stiffening stresses were summed up with the internal forces of tensile reinforcement. The principle of superposition was applied to every experimental point with increasing load and strain, resulting in the load–strain diagrams shown in Fig. 1 by dashed grey lines. Similarly to the tension stiffening relations (see Fig. 2), the difference between the modified (shrinkage-free) and experimental load–strain curves was more evident for the member with larger reinforcement ratio.

The above analysis has demonstrated that shrinkage may drastically influence the tension stiffening stress–strain relations. For this reason, removal of the shrinkage effect is essential for developing a tension stiffening law of general character.

## 5. Derivation of tension stiffening law

In a similar way as described in the previous two sections, the shrinkage-free tension stiffening relations were derived for each of the test specimen employed in the current study. Fig. 3 plots the descending branches of the shrinkage-free stress–strain tension relations obtained for all the data set. To ensure even contribution of each experimental specimen, the data set was shaped by means of an interpolation procedure described in [12]. The procedure aims at equal representation of data of the members with different material and geometrical characteristics and load levels. Using all available test data of each specimen within the load interval representing the cracking load and yield strength, tension stiffening stresses were established by Eq. (7) at certain levels of normalized strains ($\varepsilon_{ct}/\varepsilon_{cr}$ = 1.0, 1.5, 2.0, 2.5,…) obtained by linear interpolation. Here $\varepsilon_{ct}$ is the concrete mean strain and $\varepsilon_{cr} = f_{ct}/E_c$ is the cracking strain.

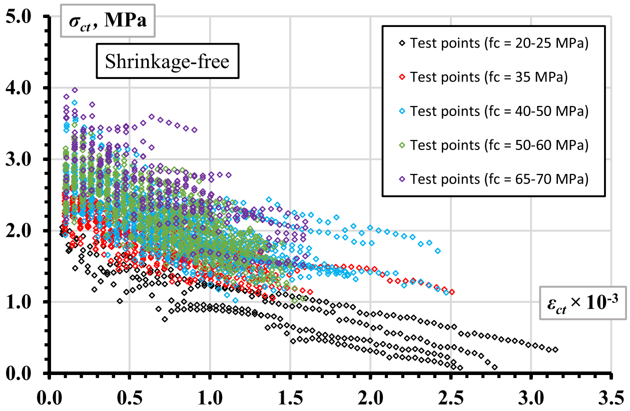

**Fig. 3.** Experimental data set for deriving shrinkage-free tension stiffening law.

The proposed tension stiffening model is shown in Fig. 4. The current study follows the traditional approach of illustrating the concrete tensile behavior in RC members by splitting the mean stress-mean strain relationship into two parts, the ascending and descending branches. The first one represents its elastic behaviour assuming that the concrete is still intact whilst the second branch examines the RC member's behavior subsequent to the surpassing of the concrete's cracking stress.

The geometry of the ascending branch will be dictated by the material's elastic constitutive law:

$$\sigma_{ct} = \varepsilon_{ct}E_c, (\varepsilon_{ct} \le \varepsilon_{ct,max}) \qquad (12)$$

The descending tension stiffening curve was obtained by means of the curve fitting using the test points given in Fig. 3. Among a wide range of possible fitting curves, the one shown in Eq. (13) has been selected as a sensible compromise between accuracy and simplicity:

$$\sigma_{ct} = 0.025 \cdot f_c - \frac{0.85 \cdot \left(\varepsilon_{ct} \cdot 10^3\right)^{0.8} - 1.5}{0.25 \cdot \left(\varepsilon_{ct} \cdot 10^3\right)^{0.3} + 0.8}, \quad (\varepsilon_{ct} \ge \varepsilon_{ct,max}) \qquad (13)$$

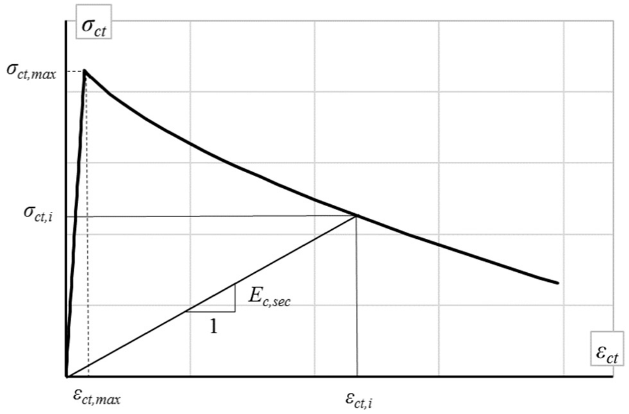

**Fig. 4.** Shrinkage-free stress–strain tension stiffening law.

In numerical modelling, the smaller value out of two $\sigma_{ct}$ calculated by Eqs. (12) and (13) for a given strain $\varepsilon_{ct}$ will be taken as the respective mean stress in the tensile concrete. If the elasticity modulus of concrete is calculated by Eurocode 2 (see Eq. (2)), the maximum stress, $\sigma_{ct,\max}$, and the respective strain, $\varepsilon_{ct,max}$, can be assessed as:

$$\sigma_{ct,max} = 0.0246f_c + 1.5372 \tag{14}$$

$$\varepsilon_{ct,max} = \sigma_{ct,max}/E_c \tag{15}$$

Fig. 5 shows the variation of the descending branches of the proposed tension stiffening law for different concrete strengths: 35 MPa, 45 MPa, 55 MPa and 65 MPa. In Fig. 6, the graphical outputs of the model are given against the test points representing different intervals of concrete strength.

A noteworthy feature of the proposed constitutive law is its relation to the compressive strength of concrete instead of the tensile strength as in most tension stiffening laws. This way the proposed model avoids the inaccuracies associated with the uncertainties related to empirical expression of the tensile strength of concrete. On the other hand, this removes the ability of using the actually measured tensile strength.

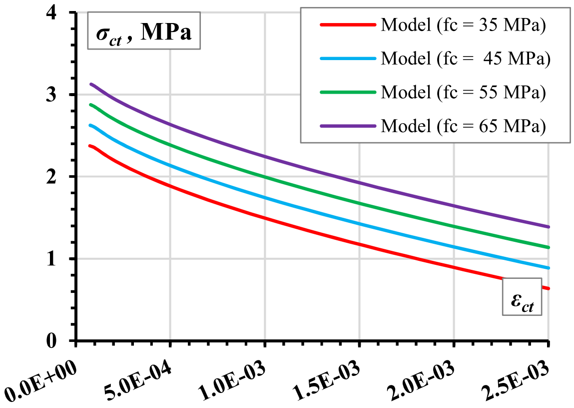

**Fig. 5.** Proposed stress–strain relationship for RC members in tension.

Fig. 7 plots the proposed law against the tension stiffening relations of Eurocode 2. The latter were derived by Eqs. (3)–(8) for two concrete grade (C35 and C55) and four reinforcement ratio (0.2%, 0.5%, 1.0% and 2.0%) levels using the load–strain diagrams defined by Eurocode 2. Both stresses and strains are normalized based on the tensile strength of concrete, $f_{ct,EC2}$, calculated by Eurocode 2.

Fig. 7 clearly demonstrates a strong dependence of the Eurocode 2 tension stiffening relations on the reinforcement ratio. This works differently in the current approach, as it seems that after removing shrinkage, tension stiffening has no or little dependence from other parameters than the compressive strength $f_c$. However, it could not be strictly concluded that reinforcement ratio or bar diameter has no influence on tension stiffening. The members with high concentration of bars in the tensile zone (characteristic to bending members with large reinforcement ratio) may undergo significant damage of concrete due to shrinkage occurring prior to external loading what might reduce the tension stiffening effect.

The tension stiffening stresses predicted by the Eurocode 2 significantly exceed the ones from the suggested model. The difference increases with the reduction in the reinforcement ratio. It can be noted that the maximum stresses of the suggested model do not reach the tensile strength of concrete ($\sigma_{ct}/f_{ct,EC2} = 1$) assessed by the Eurocode 2.

It should be kept in mind that the proposed model is shrinkage-free whereas the Eurocode 2 tension stiffening relations are affected by shrinkage. If the shrinkage effect was taken into account for the proposed model, the difference in the tension stiffening stresses from the Eurocode 2 would have been even more evident.

## 6. Validation of the proposed tension stiffening model

This section reports a limited validation analysis of the proposed tension stiffening model based on independent test data. For that tests on four RC ties (two couples of twin specimens) including the recordings of free shrinkage strain have been carried

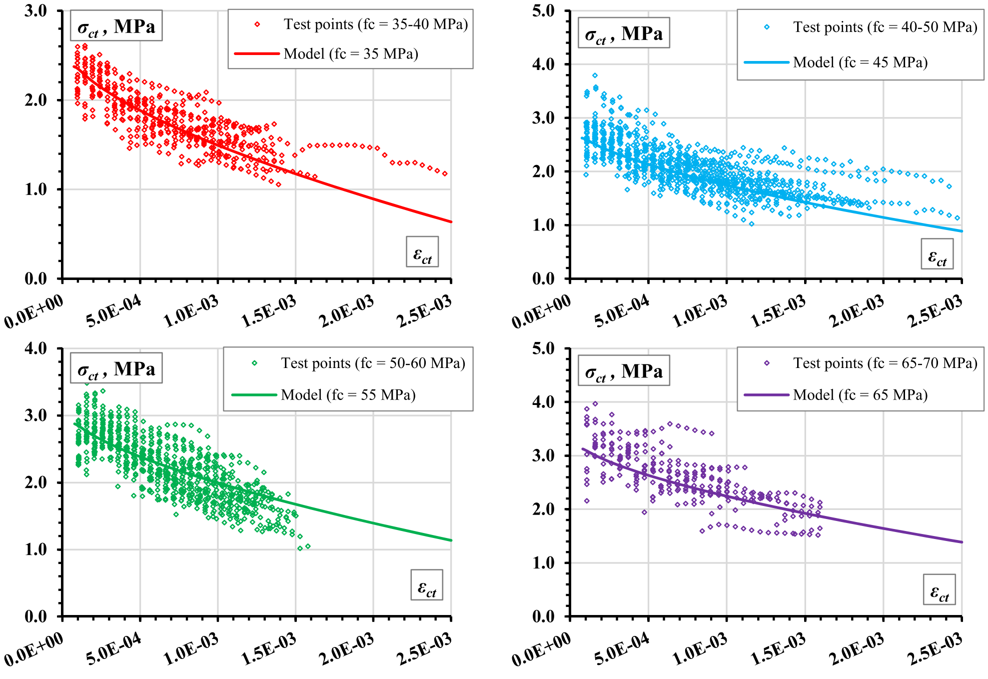

**Fig. 6.** Proposed tension stiffening law against experimental data for different ranges of concrete compressive strength.

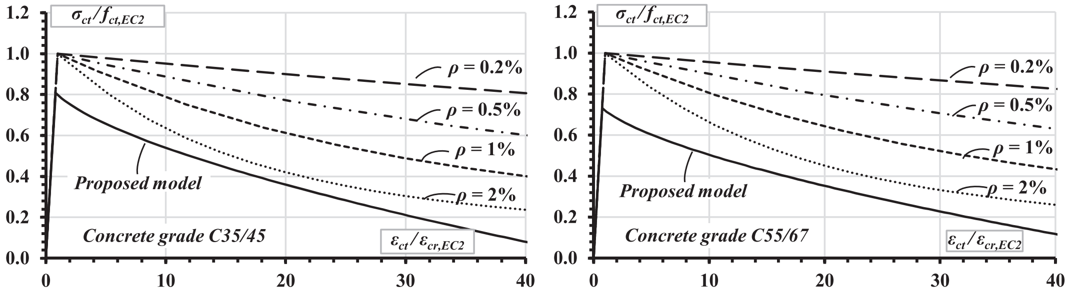

**Fig. 7.** The proposed model compared to the tension stiffening relationships obtained for Eurocode 2.

out. The predicted load–strain and tension stiffening relations were compared to the experimental ones. The technique for short-term deformation analysis of tensile RC members taking into account the shrinkage effect is described below.

### 6.1. Nonlinear stress and strain analysis of RC ties

The proposed tension stiffening model aims at providing an accurate representation of strains in RC tension members. The load–strain behaviour of cracked RC tension members can be defined by the technique reported in [17] with the inclusion of the shrinkage effect occurring prior to the external loading. The method is a non-linear iterative analysis based on the conception of secant deformation modulus taking into account varying material properties. Mean strain is calculated by this formula:

$$\varepsilon_m(t) = \varepsilon_s(t) = \varepsilon_{ct}(t) = \frac{P + P_{cs}(t)}{E_{c,sec}A_c + E_s A_s} \tag{16}$$

where $E_{c,\text{sec}}$ is the secant deformation modulus calculated for the proposed tension stiffening model. For the serviceability analysis, elastic modulus $E_s$ can be taken for reinforcement. To simplify notation, the age at first loading is omitted from the arguments of $P_{cs}(t, t_0), \varepsilon_{cs}(t, t_0)$ and $E_{ca}(t, t_0)$.

For a cracked RC member, the fictitious axial force $P_{cs}$ has a slightly different shape (compare to Eq. (8):

$$P_{cs}(t) = \bar{\varepsilon}_{cs}(t) E_{c,sec} A_c \tag{17}$$

In the above expression, the fictitious shrinkage force $P_{cs}(t)$ is considered as a short-term action. The creep and ageing effects are taken into account through the effective shrinkage strain $\bar{\varepsilon}_{cs}(t)$ assuming that shrinkage develops instantly and has the same effect on the reinforcement strain as if shrinkage was gradually increasing in time from zero to the free shrinkage strain, $\bar{\varepsilon}_{cs}(t)$. The effective shrinkage strain can be calculated by this formula [17]:

$$\bar{\varepsilon}_{cs}(t) = \varepsilon_{cs}(t) \frac{1 + \frac{E_s}{E_c(t)}\rho}{1 + \frac{E_s}{E_{ca}(t)}\rho} \tag{18}$$

In the first iterative step, the elastic modulus is taken for concrete ($E_{c,\text{sec}} = E_c$). Strain in concrete due to the acting stress is assessed as the difference between the total strain and the shrinkage strain:

$$\varepsilon_{c,\sigma}(t) = \varepsilon_{ct}(t) - \bar{\varepsilon}_{cs}(t) \tag{19}$$

For the strain $\varepsilon_{c,\sigma}$ *(t)*, the acting stress $\sigma_{ct}$ is calculated by the proposed tension stiffening law. A new value of the deformation modulus, $E_{c,\text{sec}}$, is assessed in the following way:

$$E_{c,sec} = \sigma_{ct}/\varepsilon_{c,\sigma}(t) \tag{20}$$

The latter represents the starting point of a new iteration if, compared with the $E_{c,\text{sec}}$ value from the initial or previous iteration, the agreement is not within a desired precision. In that case, the new iteration is started by inserting back in Eq. (16) the latest concrete secant elastic modulus $E_{c,\text{sec}}$.

### 6.2. Tests of RC ties and comparison to prediction results

The experimental investigation carried out at Vilnius Gediminas Technical University [35] involves four RC tension members of 1000 mm in length with 100 × 100 mm cross-section containing a single reinforcing bar of 12 or 14 mm diameter as shown in Fig. 8. Main parameters of the test ties are listed in Table 2. The following notations are defined: concrete area ($A_c$); diameter of reinforcing bar ($\varnothing$); steel area ($A_s$); steel reinforcement ratio ($\rho$); age of the specimen at the testing day ($t$); and compressive strength of 150 mm concrete cylinder ($f_c$).

The proportions of the concrete mix are given in Table 3. Portland cement and locally available crushed sandstone with a maximal nominal size of 16 mm were used as the coarse aggregate. The water/cement ratio by weight was adopted as 0.36 while the aggregate/cement ratio was 2.49. All specimens were cast using steel formwork. The specimens were demoulded two days after casting. All specimens were stored in the laboratory at an average temperature of 19.2 °C and relative humidity (RH) of 45.7%.

The concrete compressive strength was taken as the average value of three 150 mm cylinder specimens. Prior to the short-term tests of the ties, measurement of concrete shrinkage was performed on 400 × 100 × 100 mm prismatic concrete specimens having the cross-section of the experimental ties. The shrinkage recordings were performed within the 200 mm base using the surface-glued steel gauge studs. Shrinkage strain at the testing day of RC ties D12 and D14 was on average $\varepsilon_{cs} = -80.8 \cdot 10^{-6}$ and $\varepsilon_{cs} = -75.6 \cdot 10^{-6}$, respectively.

Reinforcement consisted of deformed bars (S500) with nominal diameters $\varnothing$12 and $\varnothing$14 mm. Three samples of each diameter

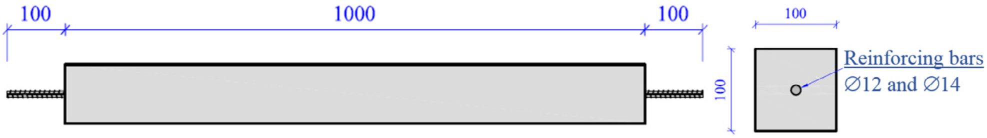

**Fig. 8.** Geometry of test RC tension members.

**Table 2**
Main characteristics of the test ties.

| Ties | $h \times b$ | $L$ | $A_c$ | $\varnothing$ | $A_s$ | $\rho$ | $t$ | $f_c$ | Steel grade |
|---|---|---|---|---|---|---|---|---|---|
| | mm | | mm$^2$ | mm | mm$^2$ | % | days | MPa | |
| *D12-1* | 100 × 100 | 1001 | 9989 | 12 | 113.1 | 1.13 | 48 | 53.1 | S500 |
| *D12-2* | | 1011 | | | | | | | |
| *D14-1* | | 1002 | 9992 | 14 | 153.9 | 1.54 | 36 | | |
| *D14-2* | | 997 | | | | | | | |

**Table 3**
Mixture proportion of the test specimens [kg/m$^3$].

| Material | Amount |
|---|---|
| Sand 0/2 mm | 280 ± 1% |
| Sand 0/4 mm | 470 ± 1% |
| Crushed aggregate 4/16 mm | 930 ± 2% |
| Cement CEM II 42.5C | 470 ± 0.5% |
| Water | 150 ± 5% |
| Concrete plasticizer *Muraplast FK 63.30* | 3.76 ± 2% |

were tested and several lengths were weighed to check the nominal size. The stresses and modulus of elasticity are based on nominal diameters. The yield stress of ∅12 and ∅14 mm steel bars was 563 MPa. Elastic modulus of reinforcing bars was obtained to be 184 GPa.

The ties were tested by applying the load to the steel bar using a displacement-controlled servo hydraulic machine with 600kN capacity (Fig. 9a). The loading rate was 0.06 mm/min. Linear variable displacement transducers (LVDT, Fig. 9b), attached to the bar and surface of the concrete were used for recording deformations. The load was measured with the electronic load cell of the testing machine (Fig. 9c).

The crack development was observed and recorded using a 50 magnification (×50) optical microscope. The test was terminated after reaching the ultimate stress in the reinforcement bar. The final crack patterns of each of the specimens are presented in Fig. 10 with the cracks numbered in the order of their appearance.

The experimental and predicted load–strain diagrams are shown in Fig. 11 separately for the twin specimens. Even though there was some difference in crack pattern for the twin specimens, the experimental load–strain relations were rather close. It demonstrates reliability of the test results. The predicted strains were also of reasonable accuracy, in the cracked stage on average reaching 93% of the test results. It should be noted that in the elastic stage the model demonstrates stiffer response compared to the experiments. The strain difference between the predicted and experimental values increases with growth of load up to the cracking point due to a rather expressed nonlinear behavior of the test ties. The reason for that is the "end effect" being responsible for the larger reinforcement strains at the ends of the member within the transfer length. Within the transfer zone which increases with growing load, strains in the reinforcement reduce progressively from the end point of the member to the point of the transfer length at which the strain compatibility is enforced. Only the central part of the member between the two points representing the transfer length, behaves based on the principles of strain compatibility and elastic theory of composites. Thus, the nonlinear effect is more clearly expressed in shorter elements as the share of the "end effect" becomes more significant.

Tension stiffening relations obtained by Eqs. (2)–(5) from the experimental and predicted load strain diagrams are given in

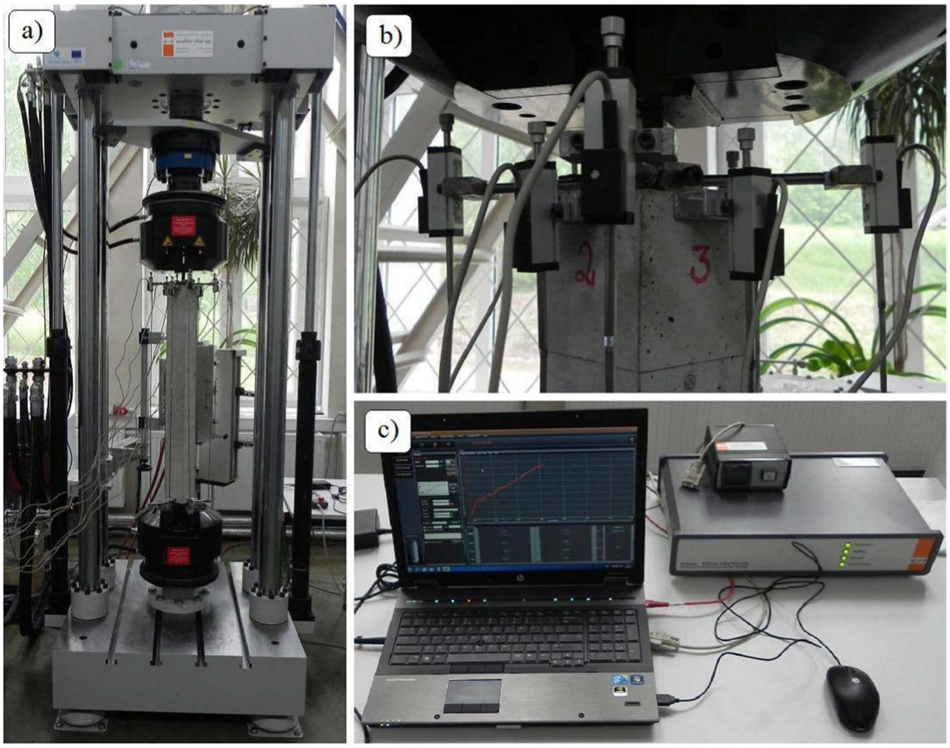

**Fig. 9.** Test setup: a) testing machine; b) layout of LVDTs; c) data acquisition equipment.

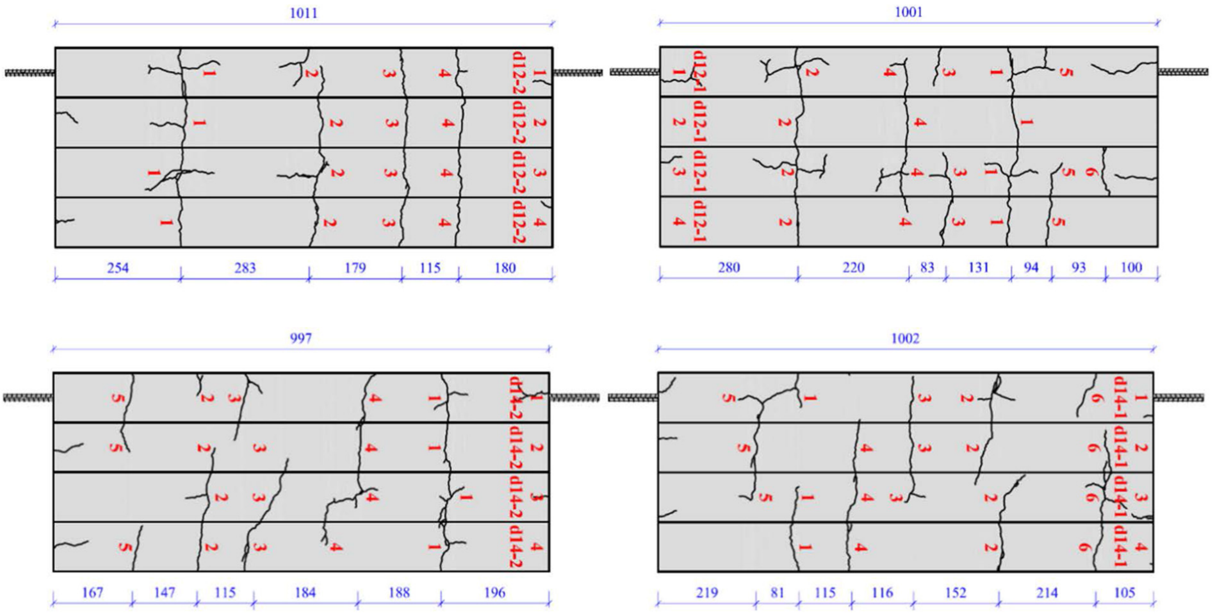

**Fig. 10.** Crack patterns of test specimens.

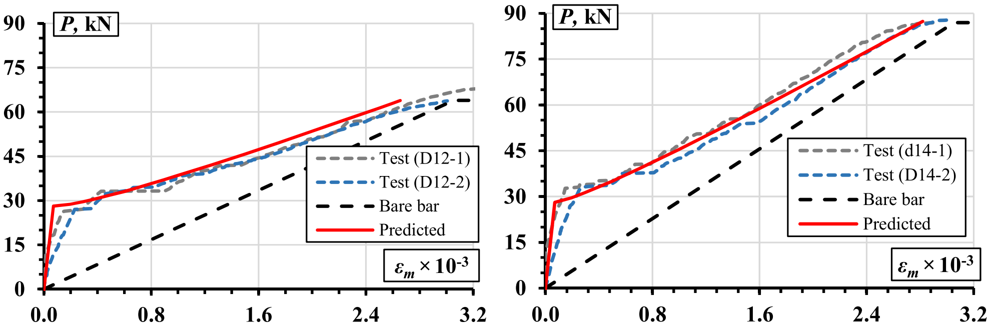

**Fig. 11.** Comparison of test and predicted load–strain diagrams.

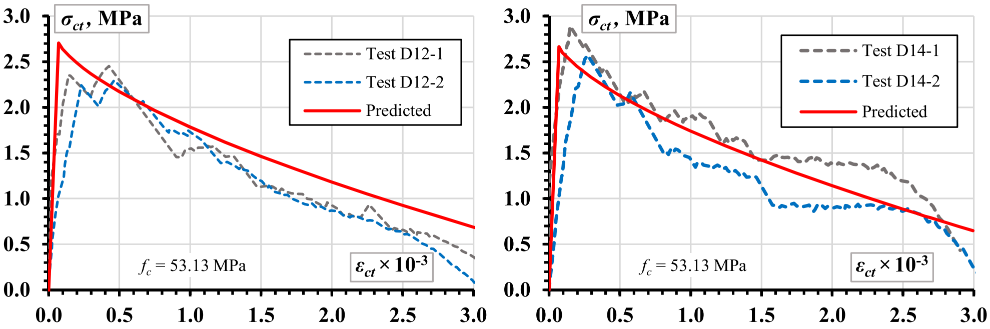

**Fig. 12.** Experimental and predicted tension stiffening stress–strain diagrams.

Fig. 12. It should be kept in mind that both the test and predicted relations are affected by shrinkage. The agreement of the curves seems adequate. Due to the "end effect", the experimental ascending branch is also having a nonlinear shape.

## 7. Concluding remarks

In this paper, a new tension stiffening law with exclusion of shrinkage effect has been developed with the goal of providing an accurate representation of strain behavior of RC tension members. Based on the current study, the following conclusions can be drawn:

1. The proposed tension stiffening model is based on the test data of seven experimental programs encompassing 108 RC tension members covering a wide range of reinforcement ratio and bar diameters as well as concrete compressive strength reaching 70 MPa. The extent of the database ensures the universal applicability of the new law.

2. The shrinkage effect occurring prior to short-term loading may drastically change the shape of tension stiffening relations obtained from the experimental load–strain diagrams of RC ties. Aside from the free shrinkage strain, reinforcement ratio is the sole most important parameter responsible for this effect.
3. Exclusion of the shrinkage effect reduces or removes the dependence of the tension stiffening stress–strain relations on reinforcement ratio. However, the current study has not provided sufficient evidence that reinforcement ratio or bar diameter has no influence on tension stiffening. The members with high concentration of bars, such as beams with large reinforcement ratio, may undergo significant damage of concrete in tension due to shrinkage occurring prior to external loading what might reduce the tension stiffening effect.
4. A limited independent validation analysis has demonstrated adequate prediction results by the proposed model.
5. The proposed constitutive law is related to the compressive strength of concrete instead of the tensile strength as in most tension stiffening laws. By this the proposed model avoids the inaccuracies associated with the uncertainties related to empirical expression of the tensile strength of concrete.
6. The tension stiffening stresses by the proposed model are significantly lower compared to the ones obtained for the Eurocode 2. The difference increases with the reduction in the reinforcement ratio.

## Conflict of interest

The authors declared that there is no conflict of interest.

## Acknowledgments

The authors gratefully acknowledge the financial support provided by the Research Council of Lithuania (project No. 09.3.3-LMT-K-712-01-0145).

## References

[1] K. Fields, P.H. Bischoff, Tension stiffening and cracking of high-strength reinforced concrete tension members, ACI Struct. J. 101 (4) (2004) 447–456.

[2] V. Gribniak, V. Cervenka, G. Kaklauskas, Deflection prediction of reinforced concrete beams by design codes and computer simulation, Eng. Struct. 56 (2013) 2175–2186.

[3] G. Kaklauskas, Crack model for RC members based on compatibility of stress transfer and mean-strain approaches, J. Struct. Eng. 143 (9) (2017) 04017105.

[4] G. Kaklauskas, R. Ramanauskas, R. Jakubovskis, Mean crack spacing modelling for RC tension elements, Eng. Struct. 150 (2017) 843–851.

[5] R.I. Gilbert, R.F. Warner, Tension stiffening in reinforced concrete slabs, J. Struct. Div. ASCE 104 (12) (1978) 1885–1900.

[6] H.Q. Wu, R.I. Gilbert, Modeling short-term tension stiffening in reinforced concrete prisms using a continuum-based finite element model, Eng. Struct. 31 (10) (2009) 2380–2391.

[7] G. Kaklauskas, J. Ghaboussi, Stress-strain relations for cracked tensile concrete from RC beam tests, J. Struct. Eng. 127 (1) (2001) 64–73.

[8] L. Torres, F. Lopez-Almansa, L.M. Bozzo, Tension stiffening model for cracked flexural concrete members, J. Struct. Eng. 130 (8) (2004) 1242–1251.

[9] P.L. Ng, J.Y.K. Lam, A.K.H. Kwan, Tension stiffening in concrete beams. Part 1: FE analysis, Proc. Inst. Civ. Eng.: Struct. Build. 163 (1) (2010) 19–28.

[10] G. Kaklauskas, V. Gribniak, Hybrid tension stiffening approach for decoupling shrinkage effect in cracked reinforced concrete members, J. Eng. Mech. 142 (11) (2016) 04016085.

[11] A. Murray, R.I. Gilbert, A. Castel, A new approach to modeling tension stiffening in reinforced concrete, ACI Struct. J. 115 (1) (2018) 127–137.

[12] V. Gribniak, H.A. Mang, R. Kupliauskas, G. Kaklauskas, Stochastic tension stiffening approach for the solution of serviceability problems in reinforced concrete: constitutive modeling, Comput.-Aided Civ. Infrastruct. Eng. 30 (2015) 684–702.

[13] Eurocode 2 (2004). CEN (European Committee for Standardization). Design of Concrete Structures: part 1-1: general Rules and Rules for Buildings. Eurocode 2, Brussels.

[14] G. Kaklauskas, V. Tamulenas, V. Gribniak, P.L. Ng, R. Kupliauskas, Tension-stiffening behaviour of reinforced concrete ties of various strength classes, in: International Conference on Performance-based and Life-cycle Structural Engineering, School of Civil Engineering, The University of Queensland, 2015, pp. 582–590.

[15] R.I. Gilbert, G. Ranzi, Time-Dependent Behaviour of Concrete Structures, CRC Press, London, 2011.

[16] P.H. Bischoff, Effects of shrinkage on tension stiffening and cracking in reinforced concrete, Can. J. Civ. Eng. 28 (3) (2001) 363–374.

[17] G. Kaklauskas, V. Gribniak, D. Bacinskas, P. Vainiunas, Shrinkage influence on tension stiffening in concrete members, Eng. Struct. 31 (6) (2009) 1305–1312.

[18] V. Gribniak, G. Kaklauskas, R. Kliukas, R. Jakubovskis, Shrinkage effect on short-term deformation behavior of reinforced concrete–when it should not be neglected, Mater. Des. 51 (2013) 1060–1070.

[19] I. Khan, A. Castel, R.I. Gilbert, Tensile creep and early-age concrete cracking due to restrained shrinkage, Constr. Build. Mater. 149 (2017) 705–715.

[20] L. Huang, J. Hua, M. Kang, A. Zhang, Influence of reinforcement configuration on the shrinkage and cracking potential of high-performance concrete, Constr. Build. Mater. 140 (2017) 20–30.

[21] A.N. Ababneh, R.Z. Al-Rousan, M.A. Alhassan, M.A. Sheban, Assessment of shrinkage-induced cracks in restrained and unrestrained cement-based slabs, Constr. Build. Mater. 131 (2017) 371–380.

[22] I. Vilanova, L. Torres, M. Baena, G. Kaklauskas, V. Gribniak, Experimental study of tension stiffening in GFRP RC tensile members under sustained load, Eng. Struct. 79 (2014) 390–400.

[23] H. Mazaheripour, J.A. Barros, J. Sena-Cruz, Tension-stiffening model for FRC reinforced by hybrid FRP and steel bars, Compos. B Eng. 88 (2016) 162–181.

[24] P.C. Miglietta, G. Grasselli, E.C. Bentz, Finite/discrete element model of tension stiffening in GFRP reinforced concrete, Eng. Struct. 111 (2016) 494–504.

[25] S.B. Kang, K.H. Tan, X.H. Zhou, B. Yang, Influence of reinforcement ratio on tension stiffening of reinforced engineered cementitious composites, Eng. Struct. 141 (2017) 251–262.

[26] M. Albitar, M.M. Ali, P. Visintin, Evaluation of tension-stiffening, crack spacing and crack width of geopolymer concretes, Constr. Build. Mater. 160 (2018) 408–414.

[27] B. Farra, J.P. Jaccoud, "Influence du béton et de l'armature sur la fissuration des structures en béton". Rapport des essais de tirants sous déformation imposée de courte durée, Lausanne: EPFL, (in French) (1993) pp. 435.

[28] H.Q. Wu, R.I. Gilbert, in: An experimental study of tension stiffening in reinforced concrete members under short-term and long-term loads". UNICIV Report No. R-449, The University of New South Wales, 2008, p. 31.

[29] K.Y. Choi, K. Maekawa, Bond behavior in RC tension members based on the change of concrete fracture characteristics with temperature, Proc. Jpn. Concr. Inst. 25 (2) (2003) 991–996.

[30] K. Noghabai, Behavior of tension member elements of plain and fibrous concrete and varying cross sections, ACI Struct. J. 97 (2) (2000) 277–284.

[31] J. Stroband, Experimental Research on the Bond Behaviour of Reinforcing Bars in Lightweight and Normal Weight Concrete, Delft University of Technology, 1991. Report 25.5-91-3/VFC (in Dutch).

[32] R.H. Scott, P.A.T. Gill, Short-term distributions of strain and bond stress along tension reinforcement, Struct. Eng. 65B (2) (1987) 39–43.

[33] M. Lorrain, O. Maurel, M. Seffo, Cracking behavior of reinforced high-strength concrete tension tension members, ACI Struct. J. 95 (5) (1998) 626–635.

[34] G. Kaklauskas, V. Gribniak, Eliminating shrinkage effect from moment curvature and tension stiffening relationships of reinforced concrete members, J. Struct. Eng. 137 (12) (2011) 1460–1469.

[35] G. Danielius, Experimental and Theoretical investigAtion of Tension Stiffening in Tensile Reinforced Concrete Members MSc thesis, Vilnius Gediminas Technical University, Lithuania (in Lithuanian), 2014.